

# Posing Constraints on the Free Parameters of a New Model of Dark Energy EoS : Responses Through Cosmological Behaviours

Promila Biswas<sup>\*1</sup>, Parthajit Roy<sup>\*\*2</sup> and Ritabrata Biswas<sup>\*3</sup>

<sup>\*</sup>*Department of Mathematics, The University of Burdwan, Golapbag Academic Complex, City : Burdwan-713104, District : Purba Bardhaman, State : West Bengal, Country : India.*

<sup>\*\*</sup>*Department of Computer Science, The University of Burdwan, Golapbag Academic Complex, City : Burdwan-713104, District : Purba Bardhaman, State : West Bengal, Country : India.*

## Abstract

Since the late 1990's observations of type Ia Supernova, our universe is predicted to experience a late time cosmic acceleration. Theoretical support to this observation were intended to be built via the proposition of a hypothetical fluid which staying inside the universe exerts negative pressure. Cosmologists have prescribed many candidates for this exotic fluid so far. In this alley, a popular method is to choose time dependent equation of state parameter  $\omega = \frac{p}{\rho}$  and to parametrize it as a function of redshift. Again some common families of such parametrizations are constructed among which different members justify different properties of observed universe. Mainly, these were model dependent studies which comprises free parameters to be constrained by different observations. In this present article, a new expression for redshift parametrization has been considered and we have constrained its free parameters for two Hubble parameter vs redshift data sets. These data sets are obtained depending on two basic methodologies known as different ages method and baryonic acoustic oscillation method. Different confidence contours for our model are located under the constraints of said data sets. Beside, different thermodynamic parameters related to the evolution of our universe are analysed. It is notified that our model indicates towards a delayed dark matter model which mimics  $EoS = -1$  phenomena at the present epoch. Deceleration parameters behavior's are studied. Outcomes for both the data sets are compared with each other.

Keywords : Dark Energy, Scale Factor, Redshift parametrization.

PACS Numbers : 98.80.-k, 95.35.+d, 95.36.+x, 98.80.Jk .

## 1 Introduction

Almost twenty years ago from now, late time cosmic acceleration was pointed out for the first time ever by the observations of two independent supernova collaborating teams [1, 2]. This has speculated that the cosmic solution is comprised of time independent, spatially homogeneous hypothetical matter density and constant positive space curvature. This need, at first, led us to the establishment of cosmological constant :  $\Lambda$  model with  $\Omega_m \approx 0.3$ ,  $\Omega_\Lambda \approx 0.7$ . This model is preferred alternative to the  $\Omega_m = 1$  scenario. Albert Einstein, in the [3], to build the first cosmological model, introduced cosmological constant term ( $\Lambda$ ) to his field equations of general relativity (GR). One can treat "Cosmological Constant" as a constant valued energy density of the vacuum [4]. As the dynamic cosmological models [5,6] were noted and cosmic expansion was discovered [7], this  $\Lambda$  term appeared as an unnecessary one. Cosmic Microwave Background (CMB) evidence for spatially flat universe [8,9], i.e., the proposition for  $\Omega_{tot} \approx 1$  was declared soon after. With  $\Omega_m \ll 1$  and  $\Omega_\Lambda = 0$ , this eliminated the free expansion theory. Scale factor  $a(t)$ , which is governed by GR, grows at an accelerating rate if the pressure  $p < \frac{1}{3}\rho$ . Another popular methodology to explain the late time cosmic acceleration was introduced where a hypothetical fluid/ energy component is assumed to exert negative pressure staying at the right hand side of Einstein's field equations. Names of different candidates for such exotic matter are coined as quintessence, phantom or dark energy (DE). Value of the equation of state  $\omega = \frac{p}{\rho}$  is taken to be negative [10,11]. Most natural existence of such energy density can be simply obtained if the cosmological constant term is reintroduced into field equations. Cosmological upper bound ( $\rho \lesssim 10^{71} GeV^4$ ) is satisfied by more than the order of hundreds if DE interpolation of  $\Lambda$  is considered [11]. Besides this  $\Lambda$ CDM model, some  $\omega$ CDM models are

<sup>1</sup>promilabiswas8@gmail.com

<sup>2</sup>roy.parthajit@gmail.com

<sup>3</sup>biswas.ritabrata@gmail.com

also famous ( $\omega$  is the DE EoS parameter). Huge discrepancies between observation and theory associated with the vacuum energy density enforces us to construct a better model. Time varying cosmological constant model [12], irreversible process of cosmological matter creation [13], Chaplygin gas family [14], redshift parametrization of the EoS parameters [15,16] etc are familiar ones. Scalar field  $\phi$  with potential  $V(\phi)$  [17] is proposed as another model. In the limit  $\frac{1}{2} \ll |V(\phi)|$ , this model acts like the cosmological constant.

$H(z)$ , the expansion rate of the universe is governed by the Friedmann equation. DE density can be written as a function of EoS  $\omega(z)$  as

$$\Omega_{DE} \frac{\rho_{DE}(z)}{\rho_{DE}(z=0)} = \Omega_{DE} \exp \left[ 3 \int_0^z \left\{ \frac{1 + \omega(z')}{1 + z'} \right\} dz' \right] = \Omega_{DE} (1 + z)^{3(1+\omega)}$$

When the present values of  $\Omega_m$ ,  $\Omega_\lambda$  and  $\Omega_{tot}$  are known, the process of measuring  $H(z)$  is based on the values  $\omega(z)$ . In GR based linear perturbation theory, the pressureless matter's density contrast  $\delta(\vec{x}, t) \equiv \frac{\rho(\vec{x}, t)}{\rho(t)} - 1$  grows in proportion to linear growth function  $G(t)$ . This is followed by the differential equation

$$\ddot{G} + 2H(z)\dot{G} - \frac{3}{2}\Omega_m H_0^2 (1+z)^3 G = 0$$

where “.” denotes differentiation with respect to  $t$ .

Upto a good approximation, logarithmic derivative of  $G(z)$  is

$$f(z) \equiv -\frac{d \ln G}{d \ln(1+z)} \approx \left[ \Omega_m (1+z)^3 \frac{H_0^2}{H^2(z)} \right]^\gamma, \quad ,$$

where relevant values of cosmological parameters [18] supports  $\gamma \approx 0.55$ .

Conventions exist there to phase constrain  $\omega(z)$  in terms of linear evaluation model,  $\omega(a) = \omega_0 + \omega_a(1-a) = \omega_p + \omega_a(a_p - a)$ , where  $a = \frac{1}{1+z}$ ,  $\omega_0$  is the value of  $\omega$  at  $z = 0$  and  $\omega_p$  is the value of  $\omega$  at pivot redshift  $z_p = a_p^{-1} = -1$ .

More general set of cosmological parameters is constructed. Some necessary parameters are :-

- (i) Dimensionless Hubble's parameter  $h = \frac{H_0}{100} \text{Kms}^{-1} \text{Mpc}^{-1}$  which determines the present day value of critical density and overall scaling of distances inferred from redshifts.
- (ii)  $\Omega_m$  and  $\Omega_{tot}$  affect expansion history and “distance-redshift” relations
- (iii) The comoving distances through that the pressure wave is able to propagate between  $t = 0$  and recombination, the sound horizon  $r_s = \int_0^{t_{rec}} \frac{C_s(t)}{a(t)} dt$  determines the physical scale for the Acoustic peaks in the CMB [21] and BAO feature in low redshift matter clustering [22].
- (iv) The quantity  $\sigma_8(z)$  represents the amplitude of matter fluctuations and scales the overall amplitude of growth measurements. These may include weak density or redshift-space distortions. Time dependent modelling of DE EoS has a particular alley named as redshift parametrization which can not be obtained from the scale field dynamics. This is because of the fact that these parametrizations are neither limited functions nor they lie in the interval defined by  $\omega = \frac{\{\frac{\phi^2}{2} - V(\phi)\}^2}{\frac{\phi^4}{4} - V(\phi)^2}$  with field potential  $V(\phi)$ . Two familiar series of redshift dependent EoS are found, viz,

**Series I :**  $\omega(z) = \omega_0 + \omega_1 \left(1 - \frac{1}{1+z}\right)^n$  and **Series II :**  $\omega(z) = \omega_0 + \omega_1 \frac{z}{(1+z)^n}$ ,  $\mathbf{n} \in \mathbb{N}$ .

Some other families such as Barboza-Alcaniz [23], Efstathiou parametrization [24, 25], ASSS parametrization [26, 27], Hannestad Mörtzell Parametrization [28], Lee Parametrization [29], Feng Shen Li Li (FSLL) Parametrization [30], Polynomial Parametrization [31, 32] can be formed in literature.

In this present article, our motive is to propose a new EoS for replicate  $\omega(z) = -1$  epoch at  $z = 0$ . We will try to constrain the free parameters of the model under the observational data. While proposing the DE EoS we take care that it does not fall in any of Series I or Series II. The model has a completely new structure depending on redshift  $z$ . We will try to show whether our model generates  $\omega(z) = -1$  epoch in the neighbourhood of  $z = 0$  or not. We wish to study the nature of fractional dimensionless density parameters for our model. We plan to study the behaviour of the deceleration parameter  $q(z)$  for the proposed model and whether phase transition-(s) from deceleration to acceleration or the converse take(s) place or not.

The article is organised as follows : In section 2 we construct the cosmological model for our newly proposed parameterization. In section 3 we constrain the model under the data sets obtained with the help of differential ages method and Baryonic Acoustic Oscillation method. Section 4 comprises studies of different cosmological parameters related to our model. Finally, we briefly discuss our findings and conclude in the last section.

## 2 Mathematical Modelling of a New Kind of Redshift Parametrization

Einstein's field equation in homogeneous and isotropic Friedmann–Lemaître–Robertson–Walker (FLRW) space time (with flat section) is written as

$$3\frac{\dot{a}^2}{a^2} = \rho_{dm} + \frac{1}{2}c\dot{\phi}^2 + V(c\phi) = \rho_{dm} + \rho_{c\phi} \quad (1)$$

and

$$2\frac{\ddot{a}}{a} + \frac{\dot{a}^2}{a^2} = -\frac{1}{2}c\dot{\phi}^2 + V(c\phi) = -p_{c\phi} \quad , \quad (2)$$

with Planck's units  $8\pi G = c = 1$ , as stated earlier,  $c\phi$  is the scalar field in natural units,  $\rho_{c\phi}$ ,  $p_{c\phi}$  and  $V(c\phi)$  are the scalar field's density, pressure and potential respectively.  $\rho_{dm}$  being the matter density.

Energy density and pressure of scalar field,  $\rho_{c\phi}$  and  $p_{c\phi}$  should have the structure as

$$\rho_{c\phi} = \frac{1}{2}c\dot{\phi}^2 + V(c\phi) \quad \text{and} \quad p_{c\phi} = \frac{1}{2}c\dot{\phi}^2 - V(c\phi) \quad . \quad (3)$$

We will write non interactive DE-darkmatter conservation equations

$$\rho_{c\phi} + 3H(\rho_{c\phi} + p_{c\phi}) = 0 \quad \text{for energy} \quad (4)$$

and

$$\rho_{dm} + 3H\rho_{dm} = 0 \Rightarrow \rho_{dm} = \rho_{dm0}a^{-3} \quad \text{for matter}, \quad (5)$$

where  $\rho_{dm0}$  denotes the current value of the matter field's energy density. Equation (4) can be rewritten as

$$\omega_{c\phi} = \frac{p_{c\phi}}{\rho_{c\phi}} = -1 - \frac{a}{3\rho_{c\phi}} \frac{d\rho_{c\phi}}{da} \quad (6)$$

Among the above equations (1), (2), (4) and (5), only three equations are likely to be independent to each other. Bianchi identities can show the derivation of the fourth equation. So, we are going to solve four independent variables. Without additional input, it is impossible to find an exact solution. We propose an ansatz for the functional form of  $\rho_{c\phi}$  as

$$\frac{1}{\rho_{c\phi}} \frac{d\rho_{c\phi}}{da} = -3 \left[ \frac{\lambda_1}{1 + ak_1} + \frac{\lambda_2(1-a)}{(1 + ak_2)^2} \right] \quad , \quad (7)$$

where  $\lambda_1$ ,  $\lambda_2$ ,  $k_1$  and  $k_2$  are constants.

Integrating, we get

$$\rho_{c\phi} = A(1 + ak_1)^{-\frac{3\lambda_1}{k_1}} (1 + ak_2)^{\frac{3\lambda_2}{k_2}} \exp \left\{ \frac{3\lambda_2(1-a)}{k_2^2(1 + ak_2)} \right\} \quad , \quad (8)$$

where  $A = \rho_{c\phi0}(1 + k_1)^{\frac{3\lambda_1}{k_1}} (1 + k_2)^{-\frac{3\lambda_2}{k_2}} \exp \left\{ -\frac{3\lambda_2}{k_2^2} \right\}$  and  $\rho_{c\phi0}$  is the present time (at  $z = 0$ ) value of the scalar field density. We observe that the density depends on three distinct functions of  $a$ . If we make  $\lambda_2 = 0$  and  $k_1 = 1$ , we see the solution will take a simple power law evolution of  $\rho_{c\phi} (\sim a^{-\lambda})$ , considered in many cosmological studies [33]. Equations (7) and (8) together give us the EoS parameter  $\omega_{c\phi}$  as a function of redshift ( $z = \frac{1}{a} - 1$ ) as

$$\omega_{c\phi(z)} = -1 + \frac{\lambda_1}{(1 + k_1) + z} + \frac{\lambda_2 z}{\{(1 + k_2) + z\}^2} \quad (9)$$

This equation even can be treated to be same of

$$\omega_{c\phi(z)} = \omega_0 + \frac{\omega_1}{\omega_2 + z} + \frac{\omega_3 z}{(\omega_4 + z)^2} \quad (10)$$

In the next section we will constrain two of the free parameters of our model, namely,  $\lambda_1$  &  $\lambda_2$  by the help of Hubble's parameter vs redshift data.

### 3 Constraining the Free Parameters for DA and BAO method :

Equation (10) depicts a new construction of DE EoS parameter. From (1), (5) and (9) we have

$$H^2 = H_0^2 \left[ \Omega_{rad0} a^{-4} + \Omega_{dm0} a^{-3} + \Omega_{c\phi0} \beta (1 + ak_1)^{-\frac{3\lambda_1}{k_1}} (1 + ak_2)^{\frac{3\lambda_2}{k_2}} \exp\left\{ \frac{3\lambda_2(1 + k_2)}{k_2^2(1 + ak_2)} \right\} \right] , \quad (11)$$

where  $\beta = (1 + k_1)^{\frac{3\lambda_1}{k_1}} (1 + k_2)^{-\frac{3\lambda_2}{k_2}} \exp\left\{ -\frac{3\lambda_2}{k_2^2} \right\}$  is a constant and  $\Omega_{dm0} = \frac{\rho_{dm0}}{3H_0^2}$ ,  $\Omega_{rad0} = \frac{\rho_{rad0}}{3H_0^2}$  and  $\Omega_{c\phi0} = \frac{\rho_{c\phi0}}{3H_0^2} = 1 - \Omega_{rad0} - \Omega_{dm0}$  represent the current values of the dimensionless density parameters for the matter, radiation and the scalar field respectively. Now we will proceed for constraining the parametrization free parameters with Hubble parameter vs redshift data. For this we must enlist the data first and mention the methods for collecting the data.

While we look through the sky, if the distance through which we see some object is shorter one, Cepheid variables are used as standard candles when the celestial distance through which we are looking at is shorter one. When the turn comes for looking at distant galaxies, type Ia Supernova explosions (SNeIa) are taken as standard candles [1, 2]. Fluctuations in visible baryonic matter's density which is caused by acoustic density waves in primordial plasma of the early universe is used as Standard rulers [34, 35]. An acoustic wave can travel through primordial plasma until it is cooled to the point where it turns to neutral atoms and the maximum distance traversed by such way is the length of the standard ruler. This oscillation's name is coined as baryon acoustic oscillation (BAO) . Since the last twenty two years, studies of cosmic microwave background (CMB) (remnant electromagnetic radiation came out of early Big Bang cosmology) have enriched the understanding of expanding universe along with the mentioned candles and rulers. These methodologies, however, do not directly constrain the Hubble's parameter. Another independent methodology is named as "cosmic chronometer approach" constructed to constrain the history of the universe's expansion [36, 37] .

In ref [38], authors have analysed about  $\approx 11,000$  massive and passive galaxies and enlisted  $H(z)$  value in the range of  $0.15 < z < 1.1$  after eight measurements with accuracy of 5 – 12%. When  $z < 0.3$ , we can find the most accurate constraints. In [19, 39–41], authors have comparatively discussed the standard probe's (like BAO and SNeIa) and cosmic chronometer. In [42], some more hubble parameter values are enlisted in the range of  $0.35 < z < 0.5$ .

A star's age can be calculated when we can analyse the spectra releasing out of it. We can take accumulation of stars, i.e., galaxies so that we can point out the ages. Thus we can observe a clock's behaviour and "this so called clock" can be observed in archival data [43], GDDS- Gemini Deep Deep Survey [44]. We use BAO signature density auto-correlation function in size method as the "standard rod". Our belief is that the entire theory is basically standing on the formation of a single "burst" [45] of almost all stars of a galaxy.

We can notice more sensitive results for  $\omega(z)$  in the differential ages (DA) case. In DA case, we must believe a clock and the dates of which may vary with the universe's age according to redshift. Spectroscopic dating of galaxy's ages provides this clock. We can write  $\frac{\Delta z}{\Delta t}$  instead of  $\frac{dz}{dt}$  based on  $\Delta t$  and  $\Delta z$ , where  $\Delta z$  is a small redshift interval and  $\Delta t$  is the age difference measurement between two passively reappear galaxies that created at the same time. So it is a more genuine method rather than age determination for galaxies [46–48]. The study of globular clusters, absolute stellar ages are more absorbent to well connected ages. Moreover, we can find the lower limit to the age of the universe with respect to absolute galaxy's ages and sort weak limitations of  $\omega(z)$ .

We can write Hubble parameter as

$$dt = -\frac{(1+z)^{-1}}{H(z)} dz$$

Applying this above to old galaxies one can obtain the value of  $H_0$ , i.e., using this method to the elliptical galaxies (in the local universe) we can evaluate the current value of Hubble constant.

Now we will form two tables for two types of  $z - H(z)$  data sets and the corresponding error terms. First 46 data sets are provided by DA method and next, 26 data sets are provided by the standard ruler method, i.e., BAO method.

Table-I : Hubble parameter  $H(z)$  with redshift and errors  $\sigma_H$  from DA method

Sl No.	$z$	$H(z)$	$\sigma(z)$	Ref. No.
1	0	67.77	1.30	[49]
2	0.07	69	19.6	[50]
3	0.09	69	12	[51]
4	0.1	69	12	[52]
5	0.12	68.6	26.2	[50]
6	0.17	83	8	[52]
7	0.179	75	4	[38]
8	0.1993	75	5	[37,38]
9	0.2	72.9	29.6	[50]
10	0.24	79.7	2.7	[53]
11	0.27	77	14	[52]
12	0.28	88.8	36.6	[50]
13	0.35	82.7	8.4	[54]
14	0.352	83	14	[38]
15	0.38	81.5	1.9	[55]
16	0.3802	83	13.5	[42]
17	0.4	95	17	[51]
18	0.4004	77	10.2	[42]
19	0.4247	87.1	11.2	[42]
20	0.43	86.5	3.7	[53]
21	0.44	82.6	7.8	[56]
22	0.44497	92.8	12.9	[42]
23	0.47	89	49.6	[37,57]

Sl No.	$z$	$H(z)$	$\sigma(z)$	Ref. No.
24	0.4783	80.9	9	[42]
25	0.48	97	60	[52]
26	0.51	90.4	1.9	[55]
27	0.57	96.8	3.4	[58]
28	0.593	104	13	[38]
29	0.6	87.9	6.1	[56]
30	0.61	97.3	2.1	[55]
31	0.68	92	8	[38]
32	0.73	97.3	7	[56]
33	0.781	105	12	[38]
34	0.875	125	17	[38]
35	0.88	90	40	[52]
36	0.9	117	23	[52]
37	1.037	154	20	[38]
38	1.3	168	17	[52]
39	1.363	160	33.6	[59]
40	1.43	177	18	[52]
41	1.53	140	14	[52]
42	1.75	202	40	[52]
43	1.965	186.5	50.4	[59]
44	2.3	224.0	8.0	[60]
45	2.34	222	7	[61]
46	2.36	226	8	[62]

Table-II : Hubble parameter  $H(z)$  with redshift and errors  $\sigma_H$  from BAO method

Sl No.	$z$	$H(z)$	$\sigma(z)$	Ref. No.
1	0.24	79.69	2.99	[53]
2	0.30	81.7	6.22	[63]
3	0.31	78.18	4.74	[64]
4	0.34	83.8	3.66	[53]
5	0.35	82.7	9.1	[65]
6	0.36	79.94	3.38	[64]
7	0.38	81.5	1.9	[55]
8	0.40	82.04	2.03	[64]
9	0.43	86.45	3.97	[53]
10	0.44	82.6	7.8	[56]
11	0.44	84.81	1.83	[64]
12	0.48	87.79	2.03	[64]
13	0.51	90.4	1.9	[55]

Sl No.	$z$	$H(z)$	$\sigma(z)$	Ref. No.
14	0.52	94.35	2.64	[64]
15	0.56	93.34	2.3	[64]
16	0.57	87.6	7.8	[66]
17	0.57	96.8	3.4	[58]
18	0.59	98.48	3.18	[64]
19	0.60	87.9	6.1	[56]
20	0.61	97.3	2.1	[55]
21	0.64	98.82	2.98	[64]
22	0.73	97.3	7.0	[56]
23	2.30	224	8.6	[60]
24	2.33	224	8.7	[67]
25	2.34	222	8.5	[61]
26	2.36	226	9.3	[62]

Using the above data for both methods, we will plot  $H(z) - z$  graphs in figure 1.

We can see the values of  $H(z)$  corresponding to the values of redshift  $z$  are semi increasing. So the resultant graph increases with respect to  $z$ . For lower redshift, BAO method estimates the higher values of  $H(z)$  than DA method. Again, for higher redshift, DA method determines the higher values of  $H(z)$  as compared to BAO method. Now we will constrain our model's parameters given in equation (10) with the help of the data of table I and II.

In fig.2(a), we have plotted the best fit values for  $\lambda_1$  and  $\lambda_2$  along with their corresponding  $1\sigma$ ,  $2\sigma$ ,  $3\sigma$  confidence contours using the data sets from table I and table II respectively. Figure 2(b) uses BAO with the data sets to constrain  $\lambda_1$  and  $\lambda_2$ . BAO and CMB along with the data sets are given figure 2(c). First we will analyse fig 2(a). For DA method, the point of best fit is denoted by "P" and  $1\sigma$ ,  $2\sigma$ ,  $3\sigma$  confidence regions are drawn in red, blue and black dashed lines respectively. For BAO method, "Q" is the best fit and the regions coloured as green, brown and red solid lines for  $1\sigma$ ,  $2\sigma$ ,  $3\sigma$  confidence contours respectively.

For both the data sets the confidence regions are of more or less elliptic structure and the semi major axis for the regions have the slope more than a right angle. However, slope of confidence contours for DA method is higher than that of BAO method. Tendency wise, high  $\lambda_1$  is supported with low  $\lambda_2$  to stay in to particular confidence region whereas low value of  $\lambda_1$  is accompanied with high  $\lambda_2$ . This signifies the DE model given in equation (9) allows either

Fig.1

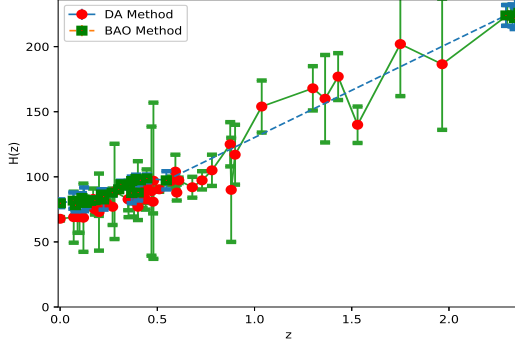


Fig. 1 :  $H(z) - z$  graph using the data set from table I and II. Red circle and green rectangle symbol indicate DA method and BAO method respectively.

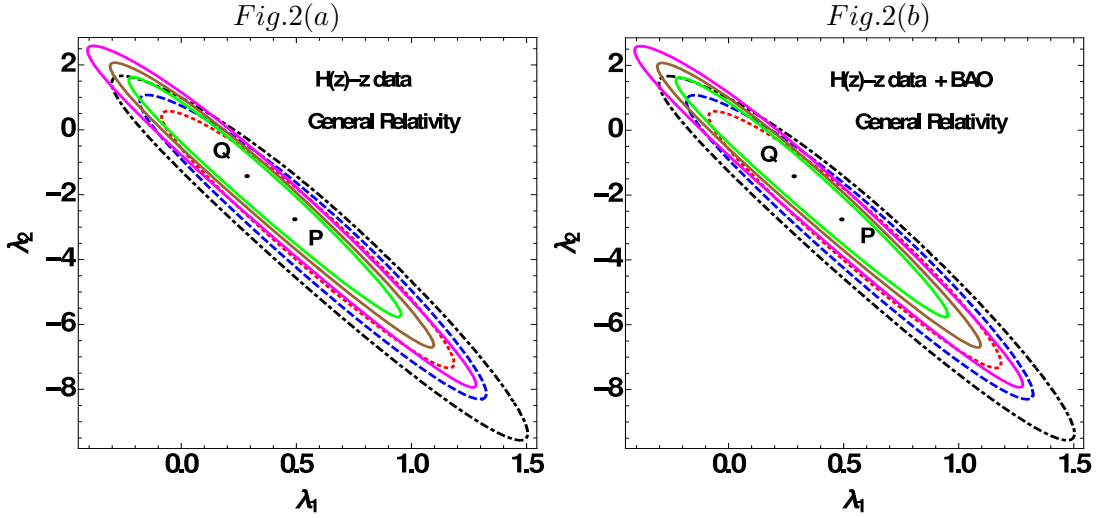


Fig.2(a)-(b) :  $1\sigma$ ,  $2\sigma$ ,  $3\sigma$  confidence contours for  $H(z) - z$  data set and  $H(z) - z + \text{BAO}$  data set

of the second or third term to dominate. At the best fits, if we take  $z = 0$ , then  $\omega(z) = -0.553388$  for DA method and  $\omega(z) = -0.741869$  for BAO method. The spans of different regions for both cases are enlisted in table - III.

Comparison shows the length of major axis for confidence contours of or BAO data (table I) is less than that for DA data (table II). So lesser amount of region is enclosed as  $1\sigma$  confidence if we consider BAO method. The maximum portion of  $1\sigma$  region of BAO is common to that of DA. So BAO method has the tendency to constrain the parameters.

In ref [34] BAO peak parameter is suggested. BAO signal at a scale of  $\sim 100Mpc$  was detected. Using the BAO peak joint analysis, here we will look into the values of  $\lambda_1$  and  $\lambda_2$  for our redshift parametrization model. We will analyse our model in the range of  $0 < z < z_1$ , where  $z_1 = 2.36$  which is called typical redshift [69] while we use SDSS data samples. BAO peak parameter is defined as

$$\mathcal{A}_{BAO} = \sqrt{\Omega_m} \left( \frac{\int_0^{z_1} E(z)^{-1} dz}{\sqrt{E(z_1)} z_1} \right)^{\frac{2}{3}}$$

For flat FLRW model,  $\mathcal{A}_{BAO} = 0.469 \pm 0.017$ . Hence, for our analysis, the  $\chi_{BAO}^2$  can be written as,

$$\chi_{BAO}^2 = \frac{(\mathcal{A}_{BAO} - 0.469)^2}{0.017^2}$$

We have plotted the figure 2(b) for  $H(z) - z$  data sets along with BAO constraint and the addition of it does not change the basic nature of the confidence curves. The best fits and regions are enlisted are in table IV. In this case  $\omega(z)|_{z=0}$  is  $-0.554712$  for DA method and  $-0.742965$  for BAO method.

CMB power spectrum's shift parameter peak is given by [70, 71]

$$\mathcal{R} = \sqrt{\Omega_m} \int_0^{z_2} \frac{dz'}{E(z')}$$

where  $z_2$  describes the value of the particular  $z$  at the last scattering surface. WMAP predicts the value of  $\mathcal{R} = 1.726 \pm 0.018$  at  $z = 1091.3$ . The  $\chi^2_{\text{CMB}}$  function (for CMB measurement) is defined as

$$\chi^2_{\text{CMB}} = \frac{(\mathcal{R} - 1.726)^2}{0.018^2}$$

We have imposed this method and have plotted the confidence contours in fig 2(c).

The best fits and the spans of confidence contour curves are mentioned in the table V. Secondly, it is noticeable that the best fits are placed in the fourth quadrant. In this case at present epoch, i.e., at  $z = 0$ ,  $\omega(z) = -1$  for DA method and  $-0.743405$  for BAO method.

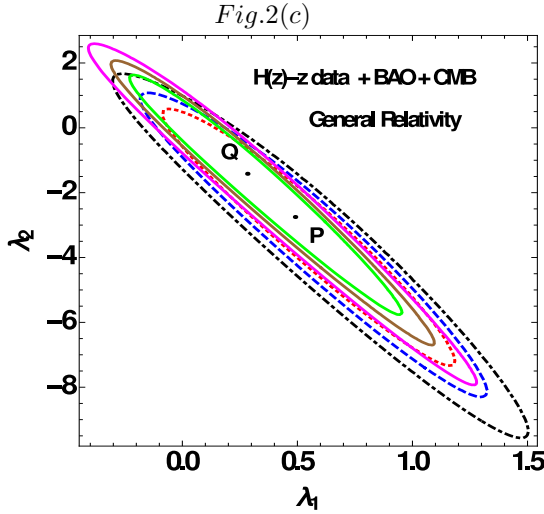


Fig.2(c) :  $1\sigma$ ,  $2\sigma$ ,  $3\sigma$  confidence contours for  $H(z) - z$  data set + BAO + CMB

As  $\omega(z)|_{z=0} = -1$  after using BAO and CMB in our model with  $H(z) - z$  data from DA method, it is significant that our cosmological model with BAO and CMB is the best measurement to support our result with  $\Lambda$ CDM model.

Table III :The best fit values of  $\lambda_1$ ,  $\lambda_2$ ,  $\chi^2$  and corresponding region of  $1\sigma$ ,  $2\sigma$  and  $3\sigma$  for both DA and BAO method using  $H(z) - z$  data set

Tools	stat. info	Region of the contours			
		DA Method		BAO Method	
$H(z) - z$ data	Best fits	$\chi^2 = 44.3734$ , $\omega(z) _{z=0} = -0.553388$		$\chi^2 = 32.346$ , $\omega(z) _{z=0} = -0.741869$	
		$\lambda_1 = 0.491273$ ( $V_{11}$ )	$\lambda_2 = -2.75766$ ( $V_{12}$ )	$\lambda_1 = 0.283944$ ( $V_{21}$ )	$\lambda_2 = -1.42732$ ( $V_{22}$ )
	$1\sigma$	$V_{11}^{+0.704727}$ $-0.587388$	$V_{12}^{+3.38546}$ $-4.64334$	$V_{21}^{+0.679856}$ $-0.52544$	$V_{22}^{+3.10732}$ $-4.42068$
	$2\sigma$	$V_{11}^{+846727}$ $-0.684273$	$V_{12}^{+3.87666}$ $-5.62634$	$V_{21}^{+0.822056}$ $-0.608144$	$V_{22}^{+3.58232}$ $-5.37068$
	$3\sigma$	$V_{11}^{+1.021727}$ $-0.800673$	$V_{12}^{+4.49166}$ $-6.85434$	$V_{21}^{+1.005056}$ $-0.702744$	$V_{22}^{+4.09432}$ $-6.61268$

Table IV :The best fit values of  $\lambda_1$ ,  $\lambda_2$ ,  $\chi^2$  and corresponding region of  $1\sigma$ ,  $2\sigma$  and  $3\sigma$  for both DA and BAO method using  $H(z) - z + \text{BAO}$  data set

Tools	stat. info	Region of the contours			
		DA Method		BAO Method	
$H(z) - z$ data + BAO	Best fits	$\chi^2 = 804.712$ , $\omega(z) _{z=0} = -0.554712$		$\chi^2 = 792.668$ , $\omega(z) _{z=0} = -0.742965$	
		$\lambda_1 = 0.489817$ ( $V_{11}$ )	$\lambda_2 = -2.75048$ ( $V_{12}$ )	$\lambda_1 = 0.282739$ ( $V_{21}$ )	$\lambda_2 = -1.4207$ ( $V_{22}$ )
	$1\sigma$	$V_{11}^{+7.06183}$ $-0.590517$	$V_{12}^{+3.373787}$ $-4.614513$	$V_{21}^{+0.681061}$ $-0.524239$	$V_{22}^{+3.1287}$ $-4.4333$
	$2\sigma$	$V_{11}^{+0.846183}$ $-0.685317$	$V_{12}^{+3.914487}$ $-5.618513$	$V_{21}^{+0.823261}$ $-0.606939$	$V_{22}^{+3.5347}$ $-5.3553$
	$3\sigma$	$V_{11}^{+1.025183}$ $-0.794917$	$V_{12}^{+4.454487}$ $-6.853513$	$V_{21}^{+1.006261}$ $-0.701539$	$V_{22}^{+4.0507}$ $-6.5723$

Table V :The best fit values of  $\lambda_1$ ,  $\lambda_2$ ,  $\chi^2$  and corresponding region of  $1\sigma$ ,  $2\sigma$  and  $3\sigma$  for both DA and BAO method using  $H(z) - z + \text{BAO} + \text{CMB}$  data set

Tools	stat. info	Region of the contours			
$H(z) - z$ data + BAO + CMB	Best fits	DA Method		BAO Method	
		$\chi^2 = 9999.38, \omega(z) _{z=0} = -1$		$\chi^2 = 9987.35, \omega(z) _{z=0} = -0.743405$	
		$\lambda_1 =$ 0.489817 ( $V_{11}$ )	$\lambda_2 =$ -2.75048 ( $V_{12}$ )	$\lambda_1 =$ 0.282254 ( $V_{21}$ )	$\lambda_2 =$ -1.4176 ( $V_{22}$ )
	1 $\sigma$	$V_{11}^{+0.700183}$ $-0.582677$	$V_{12}^{+3.38758}$ $-4.63252$	$V_{21}^{+0.523754}$ $-0.681546$	$V_{22}^{+3.0796}$ $-4.4134$
	2 $\sigma$	$V_{11}^{+0.846183}$ $-0.683817$	$V_{12}^{+3.86148}$ $-5.61952$	$V_{21}^{+0.823746}$ $-0.606454$	$V_{22}^{+3.5146}$ $-5.3554$
	3 $\sigma$	$V_{11}^{+1.016183}$ $-0.803917$	$V_{12}^{+4.41448}$ $-6.88352$	$V_{21}^{+1.006746}$ $-0.701054$	$V_{22}^{+4.0576}$ $-6.5864$

## 4 Studies of Different Cosmological Parameters of this Parameterization

:

The deceleration parameter  $q$  is defined as

$$q = -\frac{\ddot{a}}{aH^2} = -\left(1 + \frac{\dot{H}}{H^2}\right) \quad (12)$$

where  $\dot{H} = \frac{dH}{dt} = aH \frac{dH}{da}$ .

From equations (11) and (12), the expression for  $q$  in terms of scale factor  $a$  can be written as,

$$q(a) = -1 + \frac{2\Omega_{rad0}a^{-4} + \frac{3}{2}\Omega_{dm0}a^{-3} - \frac{3a}{2}\beta \Omega_{c\phi0} (1+ak_1)^{-\frac{3\lambda_1}{k_1}} (1+ak_2)^{\frac{3\lambda_2}{k_2}} \exp\left\{\frac{3\lambda_2(1+k_2)}{k_2^2(1+ak_2)}\right\}}{\Omega_{rad0}a^{-4} + \Omega_{dm0}a^{-3} + \beta \Omega_{c\phi0} (1+ak_1)^{-\frac{3\lambda_1}{k_1}} (1+ak_2)^{\frac{3\lambda_2}{k_2}} \exp\left\{\frac{3\lambda_2(1+k_2)}{k_2^2(1+ak_2)}\right\}} \times \left[ \lambda_2 (1+ak_2)^{-1} - \lambda_2 (1+k_2)(1+ak_2)^{-2} - \lambda_1 (1+ak_1)^{-1} \right] \quad (13)$$

Now, the equation (13), in terms of redshift  $z$  is

$$q(z) = -1 + \frac{2\Omega_{rad0}(1+z)^4 + \frac{3}{2}\Omega_{dm0}(1+z)^3 - \frac{3}{2(1+z)}\Omega_{c\phi0} \beta \left(\frac{1+k_1+z}{1+z}\right)^{-\frac{3\lambda_1}{k_1}} \left(\frac{1+k_2+z}{1+z}\right)^{\frac{3\lambda_2}{k_2}} \exp\left\{\frac{3\lambda_2(1+k_2)(1+z)}{k_2^2(1+k_2+z)}\right\}}{\Omega_{rad0}(1+z)^4 + \Omega_{dm0}(1+z)^3 + \Omega_{c\phi0} \beta \left(\frac{1+k_1+z}{1+z}\right)^{-\frac{3\lambda_1}{k_1}} \left(\frac{1+k_2+z}{1+z}\right)^{\frac{3\lambda_2}{k_2}} \exp\left\{\frac{3\lambda_2(1+k_2)(1+z)}{k_2^2(1+k_2+z)}\right\}} \times \left[ \lambda_2 \left(\frac{1+k_2+z}{1+z}\right)^{-1} - \lambda_2 (1+k_2) \left(\frac{1+k_2+z}{1+z}\right)^{-2} - \lambda_1 \left(\frac{1+k_1+z}{1+z}\right)^{-1} \right] \quad (14)$$

To study the situation in every direction we analyse the density parameters for the matter field ( $\Omega_{dm}$ ) and scalar field ( $\Omega_{c\phi}$ ) as,

$$\Omega_{dm}(z) = \frac{\Omega_{dm0}(1+z)^3}{\Omega_{rad0}(1+z)^4 + \Omega_{dm0}(1+z)^3 + \beta \Omega_{c\phi0} \left(\frac{1+k_1+z}{1+z}\right)^{-\frac{3\lambda_1}{k_1}} \left(\frac{1+k_2+z}{1+z}\right)^{\frac{3\lambda_2}{k_2}} \exp\left\{\frac{3\lambda_2(1+k_2)(1+z)}{k_2^2(1+k_2+z)}\right\}} \quad (15)$$

and

$$\Omega_{c\phi}(z) = \frac{\beta \Omega_{c\phi0} \left(\frac{1+k_1+z}{1+z}\right)^{-\frac{3\lambda_1}{k_1}} \left(\frac{1+k_2+z}{1+z}\right)^{\frac{3\lambda_2}{k_2}} \exp\left\{\frac{3\lambda_2(1+k_2)(1+z)}{k_2^2(1+k_2+z)}\right\}}{\Omega_{rad0}(1+z)^4 + \Omega_{dm0}(1+z)^3 + \beta \Omega_{c\phi0} \left(\frac{1+k_1+z}{1+z}\right)^{-\frac{3\lambda_1}{k_1}} \left(\frac{1+k_2+z}{1+z}\right)^{\frac{3\lambda_2}{k_2}} \exp\left\{\frac{3\lambda_2(1+k_2)(1+z)}{k_2^2(1+k_2+z)}\right\}} \quad (16)$$

Now adding (3) and (4), we can obtain,

$$\dot{c\phi}^2 = (1+z)^2 H^2 \left(\frac{dc\phi}{dz}\right)$$



$$\Rightarrow \frac{dc\phi(z)}{dz} = \pm(1+z)^{-1}\sqrt{3}\left[\frac{\lambda}{1+k_1+z} + \frac{\lambda_2 z}{(1+k_2+z)^2}\right]^{\frac{1}{2}}$$

$$\times \left[1 + \frac{\Omega_{rad0}(1+z)^4 + \Omega_{dm0}(1+z)^3}{\Omega_{c\phi0}\beta\left(\frac{1+k_1+z}{1+z}\right)^{-\frac{3\lambda_1}{k_1}}\left(\frac{1+k_2+z}{1+z}\right)^{\frac{3\lambda_2}{k_2}}\exp\left\{\frac{3\lambda_2(1+k_2)(1+z)}{k_2^2(1+k_2+z)}\right\}}\right]^{-\frac{1}{2}} \quad (17)$$

Again from equations (3) and (4), we can rewrite the potential in terms of that scalar field as,

$$V(c\phi) = \frac{1}{2}\rho_{c\phi}(1 - \omega_{c\phi}) \quad (18)$$

In terms of  $z$ , we can express  $V(z)$  as

$$V(z) = V_0\left(\frac{1+k_1+z}{1+z}\right)^{-\frac{3\lambda_1}{k_1}}\left(\frac{1+k_2+z}{1+z}\right)^{\frac{3\lambda_2}{k_2}}\exp\left\{\frac{3\lambda_2(1+k_2)(1+z)}{k_2^2(1+k_2+z)}\right\}\left(1 - \frac{\lambda_1}{2(1+k_1+z)} - \frac{\lambda_2 z}{2(1+k_2+z)^2}\right) \quad (19)$$

where ,  $V_0 = 3H_0^2\Omega_{c\phi0}\beta$ .

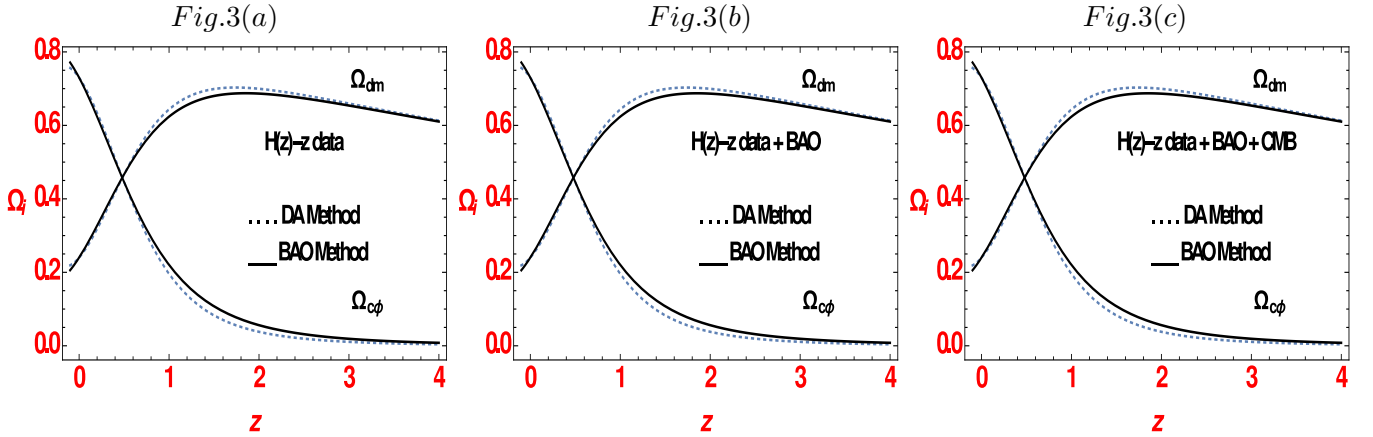


Fig.3(a)-(c) :  $\Omega_{dm}$ ,  $\Omega_{c\phi}$  vs  $z$  graphs, where dotted lines show DA method and solid lines show BAO method in the case of  $H(z) - z$  data,  $H(z) - z$  data with BAO,  $H(z) - z$  data + BAO + CMB respectively.

In figure 3(a)-3(c) we have plotted the fractional dimensionless densities  $\Omega_{dm}$  for matter and  $\Omega_{c\phi}$  for the exotic matter with respect to redshift  $z$ . In three of the cases ( $H(z) - z$  data,  $H(z) - z$  data+ BAO,  $H(z) - z$  data + BAO + CMB) respectively. We observe that the fractional densities are of increasing nature in past with more or less same slope.  $\Omega_{dm} > \Omega_{c\phi}$  for high  $z$ . But as time grows,  $\Omega_{c\phi}$  increases and after a certain point,  $z = z_1$  (say),  $\Omega_{c\phi}$  turns greater than  $\Omega_{dm}$ . These graphs, to some extent, supports the theory that in extreme part, the universe was matter dominated with  $\Lambda = 0$ . But as time grows, a delayed decay in matter world took place. This converted matter into relativistic hypothetical energy counterpart and finally  $a = -1$  epoch came to exist at the present time. This theory [72, 73] even helped a lot to bypass different theoretical discrepancies faced by  $\lambda = -1$  model alone. Fig 3(a)-(c) also depict that DA method is more appropriate than BAO to explain the transit from  $\Lambda = 0$  to  $-1$ .

We plot  $q$  as a function of  $z$  in fig 4(a)-(c).  $q$  is found to be a decreasing function with time. The rate of  $q$ 's contraction is low at high  $z$  and high at low  $z$ . We do not find any  $z$  where  $q$  changes its sign. So a transition from deceleration to acceleration is not allowed for our model. We find at least two  $z(= z_2$  and  $z_3)$ . In other domains of  $z$   $q_{BAO}(z) > q_{DA}(z)$ . The negativity of  $q(z)$  is higher at  $z = 0$  for DA method. This signifies high accelerated expansion is supported by DA method than BAO method.

In figure 5(a)-(c), we plot  $\omega_{c\phi}$  vs  $z$ . The whole curve stays in negative zone/ fourth quadrant of  $z - \omega_{c\phi}$  plane. The value of  $\omega_{c\phi}$  is decreasing for a region of high  $z$ . As  $z$  turns low,  $\omega_{c\phi}$  starts to increase and its value becomes almost equal to -1 at a little past or a small neighbourhood of present time or  $z = 0$

Fig 6(a)-(c) are plots of  $\frac{d\omega_{c\phi}}{dz}$  vs  $z$ . The rate of changes of  $\omega_{c\phi}$  with respect to  $z$  increases in high  $z$  and then it falls near the present time.

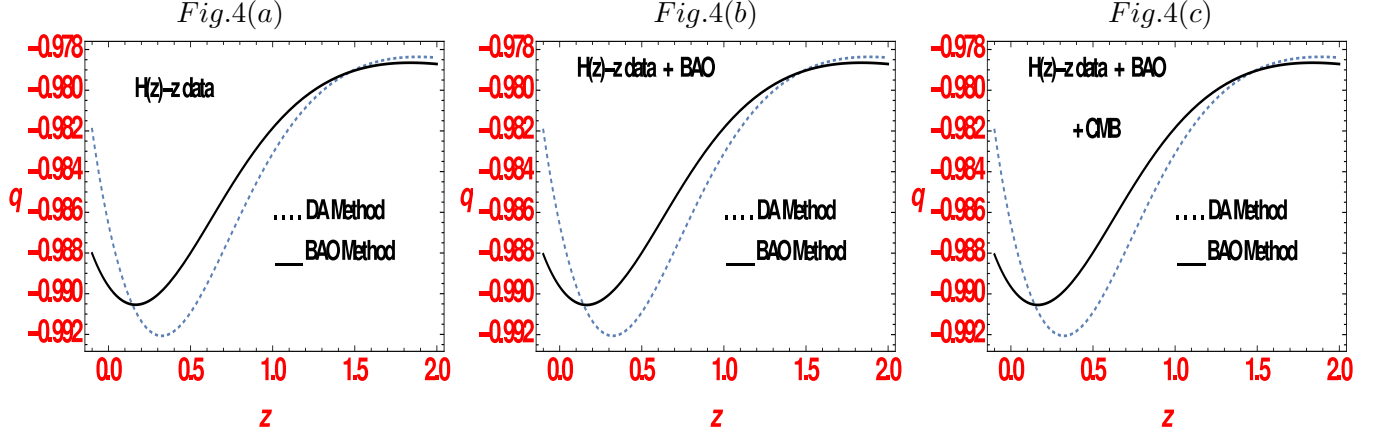


Fig.4(a)-(c) :  $q$  vs  $z$  graphs, where dotted lines are drawn for DA method and solid lines are drawn for BAO method. From fig 4(a) to 4(c) the graphs are for  $H(z) - z$  data,  $H(z) - z$  data + BAO and  $H(z) - z$  data + BAO + CMB respectively.

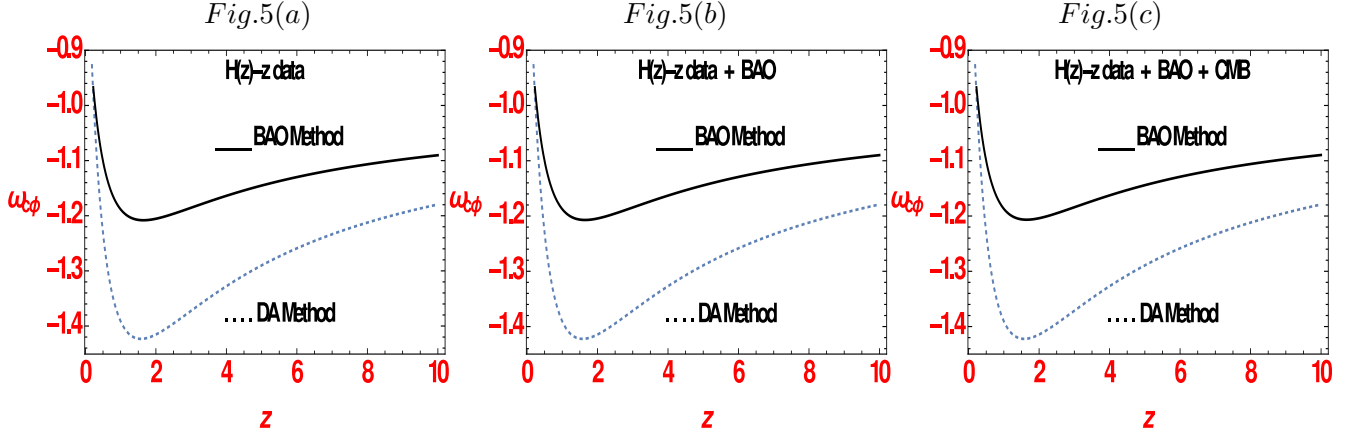


Fig.5(a)-(c) :  $\omega_{b\phi}$  vs  $z$  graphs using  $H(z) - z$  data,  $H(z) - z$  data + BAO and  $H(z) - z$  data with BAO + CMB where dotted lines shows DA method and solid line shows BAO method.

## 5 Brief Discussions and Conclusions :

This article comprises of the construction of a redshift dependent model of dark energy and this model's behaviour under the constraints given by two particular redshift-Hubble parameter data sets. We have started with a cosmological model which is mainly governed by two independent components of Einstein's field equations for FLRW metric and equation of continuity for energy and matter. We have noticed that only three among these four governing equations can be independent of each other. But we were to solve four different quantities. This is why the requirement to consider a fourth is followed. This we have done by a process which gave birth of a new equation of state for the corresponding dark energy present in the current cosmos. As we have introduced a new dark energy representative, we require to specify the values of its different parameters. To do so we have motivated ourselves to constrain the parameters for two  $H(z) - z$  data sets : derived from namely the differential ages method and Baryonic Acoustic Oscillation method. Firstly we plot these two data with each other and observe that the  $H(z)$  graph is almost increasing with respect to corresponding  $z$ . The interesting part of this graph is that the higher values of  $H(z)$  for low redshift can be seen in BAO case rather than DA method. The similar opposite phenomena happens for higher values of both redshift and  $H(z)$  in DA method compared to BAO case. Next, we locate the best fit values of two parameters of our model under the data sets obtained by DA method and BAO method (along with BAO scaling and CMB constraints). We have plotted the  $1\sigma$ ,  $2\sigma$  and  $3\sigma$  confidence contours for both data sets. We have observed that the contours are elliptic type, the semi major axis of which is inclined with a slope greater than one right angle. Confidence contours for DA method is almost a superset of that for BAO method. So BAO method constrains the

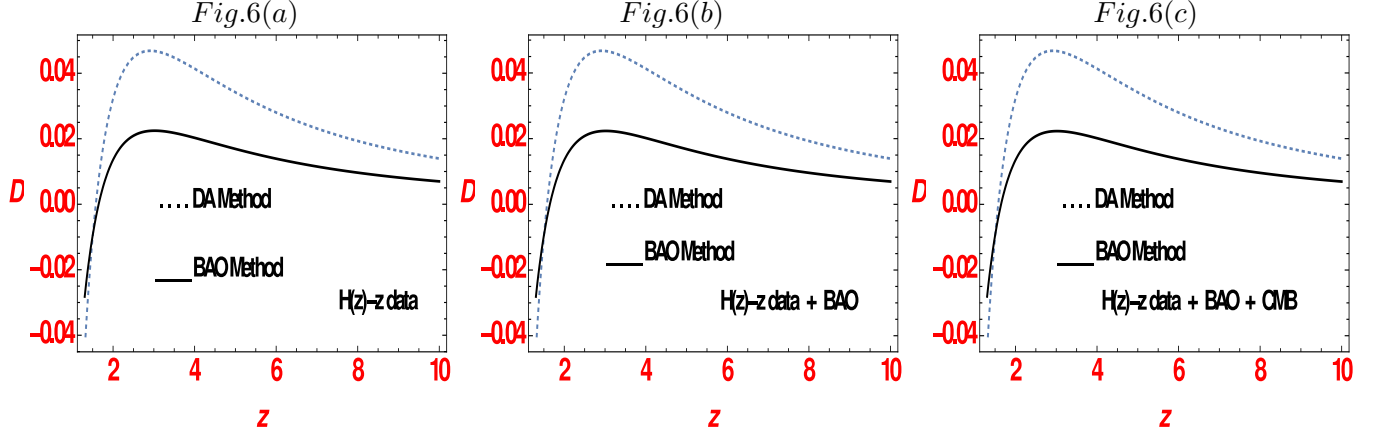


Fig.6(a)-(c) : Using  $H(z) - z$  data,  $D = \frac{d\omega_{c,\phi}}{dz}$  vs  $z$  graphs are drawn for  $H(z) - z$  data,  $H(z) - z$  data + BAO and  $H(z) - z$  data + BAO + CMB respectively, where dotted lines describes DA method and solid line describes BAO method.

model more than DA method does. We have noted down the best fits of the parameters  $\lambda_1$  and  $\lambda_2$  along with the span of the confidence contours in different tables. Fractional dimensionless densities for our model lies in the interval  $[0, 1]$  and fractional density for dark energy increases with time. On the other hand, deceleration parameter's value decreases with time.

The interesting result is found when we check the variation of the equation of state parameter with redshift. EoS parameter decreases with time and then increases again to become equal to almost  $-1$  at the past neighbourhood of present time. From our model, we can theoretically construct the algebraic structure of the deceleration parameter, fraction dimensionless density,  $\frac{d\omega_{c,\phi}(z)}{dz}$  etc. We have plotted them as well to understand the deeper insight.

Variations of fractional dimensional densities show quite interesting phenomena. We observe the fractional density of dark energy to start almost from zero at high  $z$  and to grow gradually. The same parameter for matter shows completely the opposite behaviour. For low redshift, the fractional density for dark energy grows high and almost becomes asymptotic to unity. This matches with a delayed decay of dark matter into dark energy with time.

Study of deceleration parameter vs redshift does not show any transition from deceleration to acceleration or converse. For present time neighbourhood  $q$  falls abruptly. Variation of  $\omega(z)$  shows that at present epoch  $\omega(z)$  is converging to  $-1$ , especially when  $H(z) - z$  data + BAO + CMB is applied as constraining tool.

To conclude in brief, our model which is of inverse quadratic nature fits with  $H(z)$  vs  $z$  data sets derived with the help of different ages method and Baryonic Acoustic Oscillation method by giving the best fits of the  $(\lambda_1, \lambda_2)$  type as  $(0.489817, -2.75048)$  and  $(0.282254, -1.4176)$  respectively. Both the data sets indicates to a  $\omega \sim -1$  cosmology in  $z = 0$  epoch. DA does it with a prompt jump than a slower slope of BAO. Probable decay from matter to energy in late time universe is noted.

**Acknowledgment:** This research is supported by the project grant of Government of West Bengal, Department of Higher Education, Science and Technology and Biotechnology (File no:- *ST/P/S&T/16G - 19/2017*). PB thanks Department of Higher Education, Science & Technology and Biotechnology, West Bengal for Swami Vivekananda Merit-Cum-Means Scholarship. RB thanks IUCAA, Pune for Visiting Associateship.

## References

- [1] Supernova Search Team collaboration, Riess, A.G. et al. :- “ *Observational evidence from supernovae for an accelerating universe and a cosmological constant*” *Astron. J.* **116** (1998) 1009 [astro-ph/9805201].
- [2] Supernova Cosmology Project collaboration, Perlmutter, S. et al. :- “ *Measurements of  $\Omega$  and  $\Lambda$  from 42 high redshift supernovae*” *Astrophys. J.* **517** (1999) 565 [astro-ph/9812133].
- [3] Einstein, A. :- “ *Cosmological Considerations in the General Theory of Relativity.*”; *Sitzungsber. Preuss. Akad. Wiss. Berlin (Math. Phys.)*, **142** (1917).
- [4] Zeldovich, Y.B. :- “ *Special Issue: the Cosmological Constant and the Theory of Elementary Particles.*”; *Soviet Physics Uspekhi* **11**, (1968) 381.

- [5] Friedmann, A. :- “*On the curvature of space.*” ; *Z. Phys.* **10**, (1922) 377.
- [6] Lemaitre, G. :- “*Un Univers homogène de masse constante et de rayon croissant rendant compte de la vitesse radiale des nébuleuses extra-galactiques.*; *Annales de la Société Scientifique de Bruxelles* **47**, (1927) 49.
- [7] Hubble, E. :- “*A relation between distance and radial velocity among extra-galactic nebulae.*” *Proc. Nat. Acad. Sci.* **15**, (1929) 168.
- [8] Bernardis, P. de et al.[Boomerang Collaboration] :- “*A Flat Universe from High-Resolution Maps of the Cosmic Microwave Background Radiation*” ,*Nature* **404**, (2000) 955 [arXiv:0004404v1].
- [9] Hanany, S. et al. :- “*MAXIMA-1: A Measurement of the Cosmic Microwave Background Anisotropy on angular scales of 10 arcminutes to 5 degrees*” , *Astrophys. J.* **545**, (2000) L5 [arXiv:0005123].
- [10] Peebles, P. J. E. & Ratra, B. :- “*The Cosmological Constant and Dark Energy*” , *Rev. Mod. Phys.*, **75** (2003) 559 [arXiv:0207347v2].
- [11] Biswas, P. & Biswas, R. :- “*Evolution of universe as a homogeneous system: Changes of scale factors with different dark energy Equation of States*” , *Modern Physics Letters A*, **33**, No. 19, (2018) 1850106 [arXiv:1710.06307].
- [12] Sahni, V., Starobinsky, A. A. :- “*The Case for a Positive Cosmological Lambda-term*” , *Int. J. Mod. Phys. D*, **9** (2000) 373 [arXiv:9904398v2].
- [13] Ozer, M., Taha, M. O. :- “*A possible solution to the main cosmological problems*” , *Phys. Lett. B*, **171** (1986) 363.
- [14] Biswas, P. & Biswas, R. :- “*Interacting Models of Generalized Chaplygin Gas and Modified Chaplygin Gas with Barotropic Fluid*” , *Modern Physics Letters A*, [arXiv:1805.03962].
- [15] Biswas, R. & Debnath, U. :- “*Constraining redshift parametrization parameters of dark energy: loop quantum gravity as background*” , *Eur.Phys.J.C*, **73** (2013) no.5, 2424.
- [16] Biswas,P. & Biswas, R :- “*Barboza-Alcaniz Equation of State Parametrization : Constraining the Parameters in Different Gravity Theories*” , (2018) [arXiv:1807.10608].
- [17] Ratra, B., Peebles, P.J.E.:- “*Cosmological consequences of a rolling homogeneous scalar field*” , *Phys. Rev. D* **37**, (1988) 3406.
- [18] Linder, E.V. :- “*Cosmic growth history and expansion history*” , *Phys. Rev. D* **72**, (2005) 043529 [arXiv:0507263].
- [19] Wang, X. et al.:- “*Observational constraints on cosmic neutrinos and dark energy revisited*”, *JCAP* **11** (2012) 018 [arXiv:1210.2136].
- [20] Linder, E.V. :- “*Exploring the Expansion History of the Universe*” , *Phys. Rev. Lett.*, **90** (2003) 091301 [arXiv:0208512v1].
- [21] Pan, Z., Knox, L., Mulroe, B. & Narimani, A. :- “*Cosmic Microwave Background Acoustic Peak Locations*” , *MNRAS*, **459** (2016) 2515 [arXiv:1603.03091v2].
- [22] Bassett, B. A. & Hlozek, R. :- “*Baryon Acoustic Oscillations*” , *Dark Energy*, Ed. P. Ruiz-Lapuente, (2010) [arXiv:0910.5224v1].
- [23] Barboza Jr., E. M., Alcaniz, J. S. :- “*A parametric model for dark energy*” , *Phys. Lett. B*, **666**, (2008) 415 [arXiv:0805.1713v1].
- [24] Efstathiou, G. :- “*Constraining the equation of state of the Universe from Distant Type Ia Supernovae and Cosmic Microwave Background Anisotropies*” , *Mon. Not. R. Astron. Soc.*, **310**, (1999) 842 [arXiv:9904356v1].
- [25] Silva, R., Alcaniz J. S. and Lima, J. A. S. :- it “*On the thermodynamics of dark energy*” , *Int. J. Mod. Phys. D* **16**, (2007) 469.
- [26] Alam, U., Sahni, V., Saini, T. D., Starobinski, A. A. :- “*Is there supernova evidence for dark energy metamorphosis?*” , *Mon. Not. R. Astron. Soc.*, **354** (2004a) 275 [arXiv:0311364].
- [27] Alam, U., Sahni, V., Starobinski, A. A. :- “*The case for dynamical dark energy revisited*” , *JCAP*, **0406**, (2004b) 008 [arXiv:0403687v2].
- [28] Hannestad, S., Mörtsell, E. :- “*Cosmological constraints on the dark energy equation of state and its evolution*”, *JCAP*, **0409**, (2004) 001, [arXiv:0407259].

- [29] Lee, S., :- “Constraints on the dark energy equation of state from the separation of CMB peaks and the evolution of  $\alpha$ ”, *Phys. Rev. D*, **71**, (2005) 123528 [arXiv:0504650].
- [30] Feng, C., J., Shen, X. -Y., Li, P., Li, X. -Z., :- *A New Class of Parametrization for Dark Energy without Divergence*”, *JCAP*, **1209**, (2012) 023, [arXiv:1206.0063].
- [31] Weller, J., Albrecht, A., :- “Future supernova observations as a probe of dark energy”, *Phys. Rev. D*, **65**, (2002) 103512 [arXiv:0106079].
- [32] Sendra, I., Lazkoz, R., :- “SN and BAO constraints on (new) polynomial dark energy parametrizations: current results and forecasts”, *Mon. Not. Roy. Astron. Soc.*, **422**, (2012) 776 [arXiv:1105.4943].
- [33] Copeland, E. J., Sami, M. & Tsujikawa, S. :- “Dynamics of dark energy”, *Int. J. Mod. Phys. D*, **15** (2006) 1753 [arXiv:0603057v3].
- [34] SDSS collaboration, Eisenstein, D. J. et al. :- “Detection of the baryon acoustic peak in the large-scale correlation function of SDSS luminous red galaxies”, *Astrophys. J.*, **633** (2005) 560 [arXiv:0501171].
- [35] Cole, S. et al. :- “The 2dF Galaxy Redshift Survey: power-spectrum analysis of the final data set and cosmological implications”, *Mon. Not. Roy. Astron. Soc.*, **362** (2005) 505 [arXiv:0501174].
- [36] Jimenez, R. & Loeb, A. :- “Constraining cosmological parameters based on relative galaxy ages”, *Astrophys. J.*, **573** (2002) 37 [arXiv:astro-ph/0106145].
- [37] Valent, A. G. & Amendola, L. :- “ $H_0$  from cosmic chronometers and Type Ia supernovae, with Gaussian Processes and the novel Weighted Polynomial Regression method”, *JCAP*, **1804** (2018) 051, [arXiv:2.01505v3].
- [38] Moresco, M. et al. :- “Improved constraints on the expansion rate of the Universe up to  $z \sim 1.1$  from the spectroscopic evolution of cosmic chronometers”, *JCAP*, **08** (2012) 006 [arXiv:1201.3609].
- [39] Moresco, M., Verde, L., Pozzetti, L., Jimenez, R. & Cimatti, A. :- “New constraints on cosmological parameters and neutrino properties using the expansion rate of the Universe to  $z \sim 1.75$ ”, *JCAP*, **07** (2012) 053 [arXiv:1201.6658].
- [40] Zhao, G. -B., Crittenden, R. G., Pogosian, L. & Zhang, X. :- “Examining the evidence for dynamical dark energy”, *Phys. Rev. Lett.*, **109** (2012) 171301 [arXiv:1207.3804].
- [41] Riemer-Sorensen, S., Parkinson, D., Davis, T. M. & Blake, C. :- “Simultaneous constraints on the number and mass of relativistic species”, *Astrophys. J.*, **763** (2013) 89 [arXiv:1210.2131].
- [42] Moresco, M. et al. :- “A 6% measurement of the Hubble parameter at  $z \sim 0.45$  : direct evidence of the epoch of cosmic re-acceleration”, *JCAP*, **05** (2016) 014 [arXiv:1601.01701v2].
- [43] Jimenez, R., Verde, L., Treu, T. and Stern, D. :- “Constraints on the equation of state of dark energy and the Hubble constant from stellar ages and the cosmic microwave background”, *Astrophys. J.*, **593**, (2003) 622–629, [arXiv:0302560].
- [44] McCarthy, P. J. et al :- “Evolved galaxies at  $z > 1.5$  from the Gemini Deep Deep Survey: The formation epoch of massive stellar systems”, *Astrophys. J.*, **614**, (2004) L9–L12, [arXiv:0408367].
- [45] Jimenez, R. et al :- “Premature dismissal of high-redshift elliptical galaxies”, *Mon. Not. R. Astron. Soc.*, **305**, (1999) L16–L20, [arXiv:9812222].
- [46] Dunlop, J., Peacock, J., Spinrad, H., Dey, A., Jimenez, R., Stern, D., & Windhorst, R. :- “A 3.5-Gyr-old galaxy at redshift 1.55”, *Nature*, **381**, 581 (1996).
- [47] Alcaniz, J. S. & Lima, J. A. S. :- “Dark Energy And The Epoch Of Galaxy Formation” *ApJ*, **550**, L133 (2001).
- [48] Stockton, A. :- “The Oldest Stellar Populations at  $z \sim 1.5$ ”, to be published in *Astrophysical Ages and Time Scales*, ASP Conference Series, (2001) [arXiv:0104191].
- [49] Macaulay, E. et. al. (DES collaboration) :- “First Cosmological Results using Type Ia Supernovae from the Dark Energy Survey: Measurement of the Hubble Constant”, [arXiv:1811.02376].
- [50] Zhang, C., Zhang, H., Yuan, S., Zhang, T. -J. & Sun, Y. -C. :- “Four new observational  $H(z)$  data from luminous red galaxies in the Sloan Digital Sky Survey data release seven”, *Res. Astron. Astrophys.*, **14**, 1221 (2014) [arXiv:1207.4541].

- [51] Simon, J., Verde, L. & Jimenez, R. :- “Constraints on the redshift dependence of the dark energy potential” , *Phys. Rev. D*, **71** 123001 (2005) [arXiv:0412269].
- [52] Stern, D. et al. :- “Cosmic chronometers: constraining the equation of state of dark energy. I:  $H(z)$  measurements” , *JCAP*, **1002** (2010) 008 [arXiv:0907.3149].
- [53] E. Gaztañaga, A. Cabré and L. Hui :- “Clustering of luminous red galaxies - IV. Baryonacoustic peak in the line-of-sight direction and a direct measurement of  $H(z)$ ” , *Mon. Not. R.Astron. Soc.*, **399** (2009) 1663 [arXiv:0807.3551]
- [54] Chuang, C. H. & Wang, Y., :- “Modeling the anisotropic two-point galaxy correlation function on small scales and improved measurements of  $H(z)$  from the Sloan Digital Sky Survey DR7 luminous red galaxies” , *Mon. Not. R. Astron. Soc.*, **435** (2013) 255 [arXiv:1209.0210].
- [55] Alam, S., et al. :- “The clustering of galaxies in the completed SDSS-III Baryon Oscillation Spectroscopic Survey: cosmological analysis of the DR12 galaxy sample” , (2016), [arXiv:1607.03155]
- [56] Blake, C. et al. :- “The WiggleZ Dark Energy Survey: joint measurements of the expansion and growth history at  $z \leq 1$ .” , *Mon. Not. R. Astron. Soc.*, **425** (2012) 405 [arXiv:1204.3674].
- [57] Ratsimbazafy, A. L. et al. :- “Age-dating Luminous Red Galaxies observed with the Southern African Large Telescope” , *Mon. Not. Roy. Astron. Soc.*, **467** (2017) 3239 [arXiv:1702.00418].
- [58] Anderson, L. et al. [BOSS Collaboration] :- “The clustering of galaxies in the SDSS-III Baryon Oscillation Spectroscopic Survey: baryon acoustic oscillations in the Data Releases 10 and 11 Galaxy samples.” , *Mon. Not. R. Astron. Soc.*, **441(1)** (2014) 24 [arXiv:1312.4877].
- [59] Moresco, M. :- “Raising the bar: new constraints on the Hubble parameter with cosmic chronometers at  $z \sim 2$ ” , *Mon. Not. Roy. Astron. Soc.*, **450** (2015) L16 [arXiv:1503.01116].
- [60] N. G. Busca, T. Delubac, J. Rich, et al. :- “Baryon acoustic oscillations in the Ly alpha forest of BOSS quasars” , *Astron. & Astrophys.*, **552** (2013) 18 [arXiv:1211.2616].
- [61] Delubac, T. et al. [BOSS Collaboration], “Baryon acoustic oscillations in the Ly forest of BOSS DR11 quasars” , *Astron. Astrophys.*, **574** (2015) A59 [arXiv:1404.1801].
- [62] Font-Ribera, A., et al. :- “Quasar-Lyman  $\alpha$  Forest Cross-Correlation from BOSS DR11 : Baryon Acoustic Oscillations” , *JCAP*, **1405**, (2014) 027 [arXiv:1311.1767].
- [63] Oka A. et al.:- “Simultaneous constraints on the growth of structure and cosmic expansion from the multipole power spectra of the SDSS DR7 LRG sample” , *Mon. Not. Roy. Astron. Soc.*, **439**, (2014) 2515-2530 [arXiv:1310.2820].
- [64] Wang Y. et al. :- “The clustering of galaxies in the completed SDSS-III Baryon Oscillation Spectroscopic Survey: tomographic BAO analysis of DR12 combined sample configuration space , *Mon. Not. Roy. Astron. Soc.*, **469**, (2017) 3762–3774 [arXiv:1607.03154].
- [65] Chuang C.H. and Wang Y. “Modeling the Anisotropic Two-Point Galaxy Correlation Function on Small Scales and Improved Measurements of  $H(z)$ ,  $DA(z)$ , and  $f(z)\sigma_8(z)$  from the Sloan Digital Sky Survey DR7 Luminous Red Galaxies” , *Mon. Not. Roy. Astron. Soc.*, **435**, (2013) 255-262 [arXiv:1209.0210].
- [66] Chuang C-H. et al. “The clustering of galaxies in the SDSS-III Baryon Oscillation Spectroscopic Survey : single-probe measurements and the strong power of  $f(z)\sigma_8(z)$  on constraining dark energy” , *Mon. Not. Roy. Astron. Soc.*, **433**, (2013). 3559-3571 [arXiv:1303.4486].
- [67] Bautista J. E. et al. :- “Measurement of baryon acoustic oscillation correlations at  $z = 2.3$  with SDSSDR12 Ly $\alpha$ -Forests” , *Astron. Astrophys.*, **603**, (2017) 23 [arXiv:1702.00176].
- [68] Lima, J. A. S., Alcaniz, J. S. :- “Flat FRW Cosmologies with Adiabatic Matter Creation: Kinematic tests” , *Astron. Astrophys.*, **348**, (1999) 1 [arxiv:9902337].
- [69] Doran, M., Stern, S. and Thommes, E. :- “Baryon acoustic oscillations and dynamical dark energy” , *JCAP*, **0704**, (2007) 015 [arXiv:0609075].
- [70] Elgaroy, O. and Multamaki, T. :- “On using the cosmic microwave background shift parameter in tests of models of dark energy” , *Astron. Astrophys.*, **471** (2007) 65E [arXiv:0702343].

- [71] Efstathiou, G. and Bond J. R. :- “*Cosmic confusion: degeneracies among cosmological parameters derived from measurements of microwave background anisotropies*” , *MNRAS*, **304**, (1999) 75 [arXiv:9807103].
- [72] Turner, M. S., Steigman, G. & Krauss, L. M. :- “*Flatness of the Universe: Reconciling Theoretical Prejudices with Observational Data*” , *Phys. Rev.Lett.*, **52**, (1984) 2090.
- [73] Mathews, G. J., Lan, N. Q. & Kolda, C. :- “*Late decaying dark matter, bulk viscosity, and the cosmic acceleration*” , *Phys. Rev. D*, **78**, (2008) 043525 [arXiv:0801.0853].